

Stepwise Radial Complexation of Organic Molecules and Organic–Metal Hybrid Assembly in Dendritic Polyphenylazomethines

Atunobu Fujii, Yousuke Ochi, Reina Nakajima, and Kimihisa Yamamoto*

Department of Chemistry, Faculty of Science and Technology, Keio University, Yokohama 223-8522

(Received January 20, 2009; CL-090068; E-mail: yamamoto@chem.keio.ac.jp)

We found that triphenylmethyl cation tetrafluoroborate ($\text{TPM}^+\text{BF}_4^-$) could be coordinated to the imine group of dendritic phenylazomethine (DPA) in stepwise radial fashion, which allows for control of the number and position of TPM and metals incorporated into the dendrimers. Organic–metal hybrid assembly was also achieved.

Dendrimers¹ are highly branched organic macromolecules which have a single molecular weight. They have been noted as a possible building block for fabricating new nanomaterials. These dendrimers contain nanosized space in the center into which functional substances can be incorporated to give capsules which can be used as metal catalysts,² drug delivery systems,³ etc. Many researchers have investigated incorporation via coordinate bonds, ionic bonds, or hydrophobic interactions, but it has been difficult to incorporate organic molecules quantitatively into the dendrimer because a random statistical distribution is obtained. We reported precise assembly of metal ions on dendritic phenylazomethine (DPA, Chart 1a),⁴ which is connected to novel electronic materials.⁵ In contrast to metal-ions assembly, the incorporation of organic species allows for application of the resulting species in the formation of new nanomaterials, taking advantage of the flexibility and functionality of these materials.

In this study, the organic species used was triphenylmethyl cation (TPM^+ , Chart 1b), which contains a central carbocation stabilized by delocalization over three phenyl rings. We found that TPM^+ could be coordinated to the imine group of DPA in stepwise radial fashion, which allows for control of the number and position of TPM^+ incorporated into a dendrimer.

It has been reported that triphenylmethyl cation (TPM^+) can coordinate to a pyridine nitrogen atom.⁶ This complexation behavior was observed by carrying out a titration in which triphenylmethyl tetrafluoroborate ($\text{TPM}^+\text{BF}_4^-$) was added to the imine sites of 4th generation DPA (DPAGX, designed as GX, where X is the generation number), which has

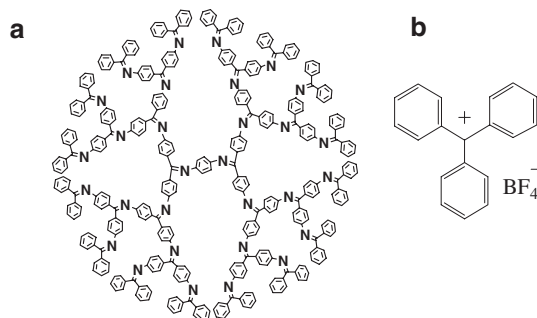


Chart 1. Structure of (a) 4th generation DPA (DPAG4) and (b) triphenylmethyl cation tetrafluoroborate ($\text{TPM}^+\text{BF}_4^-$).

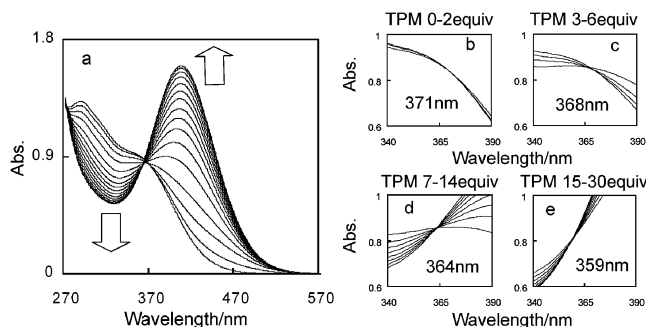
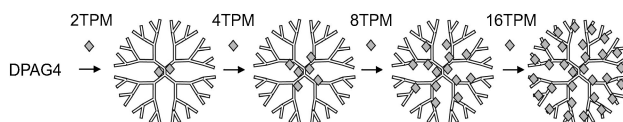


Figure 1. (a) UV–vis spectra of DPAG4 complexed with 0–30 equivalents of TPMBF_4 and isosbestic points during the addition of 0–2 equivalents (b), 3–6 equivalents (c), 7–14 equivalents (d), and of 15–30 equivalents (e) of TPMBF_4 .

30 imine sites (Chart 1a), using UV–vis spectroscopy to monitor the progress of the reaction until an equimolar amount of TPM^+ had been added. It was observed that the absorption around 445 nm increased while the absorption around 310 nm attributed to imine decreased (Figure 1a). This behavior matches that of metal ions such as FeCl_3 ⁷ or SnCl_2 ⁴ undergoing complexation with imine sites. A Job plot showed DPAG0 (Chart S1a¹²) forms a 1:1 complex with $\text{TPM}^+\text{BF}_4^-$ (Figure S1).¹² The disappearance of yellow color ($\lambda_{\text{max}} = 405$ and 435 nm) attributed to TPM carbocation by adding DPAG0 also supported the complexation (Figure S2).¹²

Stepwise radial complexation based on the electron gradient, which was explained by ca. 100 times difference between the complexation constants of neighboring DPA layers.⁸ Stepwise radial complexation of $\text{TPM}^+\text{BF}_4^-$ on DPAG4 (Scheme 1) was confirmed by UV–vis spectroscopy. An isosbestic point appears when one compound is quantitatively transformed into another by complexation.¹² Four changes in the position of the isosbestic points were observed during addition of $\text{TPM}^+\text{BF}_4^-$ to DPAG4, which indicated that four different complexations are successively formed upon $\text{TPM}^+\text{BF}_4^-$ addition (Figure 1a). These shifts are very similar to those observed during complexation of metal ions. The spectra of DPAG4 changed gradually with an isosbestic point at 371 nm observed up to the addition of 2 equivalents of $\text{TPM}^+\text{BF}_4^-$ (Figure 1b), but shifted to 368 nm between 3 and 6 equivalents (Figure 1c). During the addition of 7–14 equivalents, an isosbestic point appeared at 364 nm (Figure 1d), which moved to 359 nm (Figure 1e) during



Scheme 1. Schematic representation of the stepwise complexation of DPAG4 with TPMBF_4 .

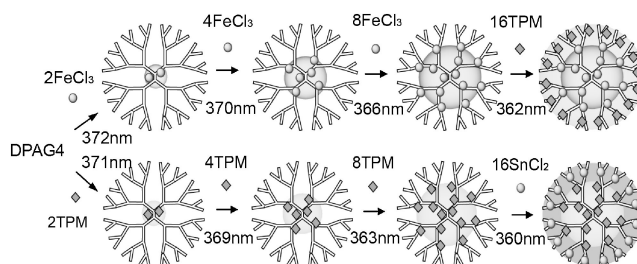
addition of 15–30 equivalents. The number of equivalents of $\text{TPM}^+\text{BF}_4^-$ required to induce a shift was commensurate with the number of imine sites present in each generation layer of DPAG4. Similar stepwise complexation was observed for DPAG2 and DPAG3 (Figure S3).¹² For DPAG2, two isosbestic points appeared at 343 and 360 nm when adding 0–2 and 3–6 equivalents of TPMBF_4 , respectively. In case of DPAG3, three isosbestic points centred at 373, 361, and 355 nm appeared when adding 0–2, 3–6, and 7–14 equivalents of TPMBF_4 , respectively.

The complexation of DPA with $\text{TPM}^+\text{BF}_4^-$ was observed using ^1H NMR and ^{13}C NMR spectra (Figure S4).¹² Complexation of DPAG0 with $\text{TPM}^+\text{BF}_4^-$ was observed. The carbon peak of imine site (C_1 , DPAG0) shifted from 167 to 179 ppm on addition of an equimolar amount of $\text{TPM}^+\text{BF}_4^-$ (Figure S4B).¹² This is probably because of the drop in π electron density of the imine site due to the complexation. After complexation, a new peak appeared at 81 ppm, this was identified as the quaternary carbon of TPM coordinated to the nitrogen of imine (C_2), which correspond to the neutralization of the TPM carbocation by a DPA imine. The number of peaks for the complex was equal to the sum of the peaks of DPAG0 and TPM^+ . Comparison of the ^1H NMR spectra of DPAG0 with those of DPAG0 after addition of an equimolar amount of $\text{TPM}^+\text{BF}_4^-$ shown that all the peaks of the DPAG0 shifted down field due to the electron-withdrawing effect of $\text{TPM}^+\text{BF}_4^-$ (Figure S4A).¹²

In terms of molecular size, $\text{TPM}^+\text{BF}_4^-$ is larger than both FeCl_3 and SnCl_2 , but it can form an assembly with DPA because the DPA skeleton is rigid and has enough space to incorporate molecules. The percentage free volume (V_{free}) in the DPAG4 was determined to be 74% based on van der Waals volume (V_{VW}) which was calculated using Edward's increments and the hydrodynamic volume (V_{h}) which was calculated using the hydrodynamics radius (Figure S5).^{9,12} Thus, it is larger than a Fréchet type dendrimer. It was estimated that upon coordination of 30 equiv of TPM^+ and BF_4^- to DPAG4 free space would reduce to about 30%. It was previously reported that the free space of Fréchet type G4 dendrimer was 21%.¹⁰ Thus, 30 equiv of TPM^+ and BF_4^- can be incorporated into DPAG4.

Organic–metal hybrid assembly can be achieved by taking advantage of the difference in the complexation constant to DPA imines, K ($K_{\text{Fe}} > 10^8 \text{ M}^{-1}$, $K_{\text{TPM}} = 5 \times 10^6 \text{ M}^{-1}$, and $K_{\text{Sn}} = 10^4 \text{ M}^{-1}$). In the previous study, we reported that heterometal assembling on DPA appears to be governed by the complexation ability of metal salts, with stronger coordinating metal in the inner layer and the weaker coordinating metals in the outer layer.¹¹ The complexation abilities of three acids, that is, FeCl_3 , TPMBF_4 , and SnCl_2 , were compared by the normalized titration curve of DPAG1 in $\text{THF}/\text{CH}_3\text{CN} = 1:1$ solution (Figure S6).¹² The complexation ability for $\text{TPM}^+\text{BF}_4^-$ was smaller than that of FeCl_3 , but larger than that of SnCl_2 . The results confirmed that the order of complexation ability was as follows: $\text{FeCl}_3 > \text{TPMBF}_4 > \text{SnCl}_2$.

We demonstrated UV–vis titration by the addition of FeCl_3 followed by TPMBF_4 using DPAG4 (Scheme 2, Figure S7,¹² and Table S1¹²). After adding 14 equiv of FeCl_3 , the isosbestic points were observed at 372 nm for 0–2 equiv of FeCl_3 , 370 nm for 3–6 equiv, and 366 nm for 7–14 equiv, which correspond to the complexation of 1st–3rd layers. After adding TPMBF_4 , the isosbestic points shifted to 362 nm for 0–16 equiv of TPMBF_4 , which corresponded to the complexation of 4th layers. It confirmed that



Scheme 2. Image of the organic–metal hybrid assembly and its isosbestic points on DPAG4 using TPMBF_4 , FeCl_3 , and SnCl_2 .

the inner layer of DPAG4 was complexed with FeCl_3 , followed by the outer layer with $\text{TPM}^+\text{BF}_4^-$.

We also performed the addition of TPMBF_4 followed by SnCl_2 (Scheme 2, Figure S8, and Table S1).¹² After adding 14 equiv of TPMBF_4 , the isosbestic points were observed at 371 nm for 0–2 equiv of TPMBF_4 , 369 nm for 3–6 equiv, and 363 nm for 7–14 equiv, which correspond to the complexation of 1st–3rd layers. After that, the isosbestic points shifted to 360 nm for the following 0–16 equiv of SnCl_2 , which means the complexation of 4th layers. These unique complexations expand the variation of precise metal assembly based on the complexation constants of different species.

It was found that $\text{TPM}^+\text{BF}_4^-$ could be precisely assembled in DPA. This is a novel method which allows control of the number and location of organic molecules incorporated into dendrimers. By expanding the range of molecules that can be assembled in DPA to include organic molecules as well as metal ions, we have taken a step toward the design of novel nanomaterials.

References and Notes

- a) G. R. Newkome, Z. Yao, G. R. Baker, V. K. Gupta, *J. Org. Chem.* **1985**, *50*, 2003. b) D. A. Tomalia, H. Baker, J. Dewald, M. Hall, G. Kallos, S. Martin, J. Roeck, J. Ryder, P. Smith, *Polym. J.* **1985**, *17*, 117.
- R. M. Crooks, M. Zhao, L. Sun, V. Chechik, L. K. Yeung, *Acc. Chem. Res.* **2001**, *34*, 181.
- A. V. Ambade, E. N. Savariar, S. Thayumanavan, *Mol. Pharm.* **2005**, *2*, 264.
- a) K. Yamamoto, M. Higuchi, S. Shiki, M. Tsuruta, H. Chiba, *Nature* **2002**, *415*, 509. b) M. Higuchi, M. Tsuruta, H. Chiba, S. Shiki, K. Yamamoto, *J. Am. Chem. Soc.* **2003**, *125*, 9988. c) O. Enoki, T. Imaoka, K. Yamamoto, *Org. Lett.* **2003**, *5*, 2547.
- a) J.-S. Cho, K. Takanashi, M. Higuchi, K. Yamamoto, *Synth. Met.* **2005**, *150*, 79. b) X. Yan, T. Goodson, T. Imaoka, K. Yamamoto, *J. Phys. Chem. B* **2005**, *109*, 9321. c) T. Nishiumi, Y. Nomura, Y. Chimoto, M. Higuchi, K. Yamamoto, *J. Phys. Chem. B* **2004**, *108*, 7992.
- a) Y. Okamoto, Y. Shimakawa, *J. Org. Chem.* **1970**, *35*, 3752. b) A. R. Katritzky, C. H. Watson, Z. Dega-Szafran, J. R. Eyler, *J. Am. Chem. Soc.* **1990**, *112*, 2471.
- R. Nakajima, M. Tsuruta, M. Higuchi, K. Yamamoto, *J. Am. Chem. Soc.* **2004**, *126*, 1630.
- K. Yamamoto, M. Higuchi, A. Kimoto, T. Imaoka, K. Masachika, *Bull. Chem. Soc. Jpn.* **2005**, *78*, 349.
- a) T. Imaoka, R. Tanaka, K. Yamamoto, *Chem.—Eur. J.* **2006**, *12*, 7328. b) J. Edward, *J. Chem. Educ.* **1970**, *47*, 261.
- M. S. Matos, J. Hofkens, W. Verheijen, F. C. D. Schryver, S. Hecht, K. W. Pollak, J. M. J. Fréchet, B. Forier, W. Dehaen, *Macromolecules* **2000**, *33*, 2967.
- K. Takanashi, A. Fujii, R. Nakajima, H. Chiba, M. Higuchi, Y. Einaga, K. Yamamoto, *Bull. Chem. Soc. Jpn.* **2007**, *80*, 1563.
- Supporting Information is available electronically on the CSJ-Journal Web site, <http://www.csj.jp/journals/chem-lett/index.html>.